Joint EUROGRAPHICS - IEEE TCVG Symposium on Visualization (2004)
O. Deussen, C. Hansen, D.A. Keim, D. Saupe (Editors)

Boundary Switch Connectors for Topological Visualization of Complex 3D Vector Fields

T. Weinkauf[1], H. Theisel[2], H.-C. Hege[1] and H.-P. Seidel[2]

[1] Zuse Institute Berlin (ZIB), Berlin, Germany — {weinkauf, hege}@zib.de
[2] MPI Informatik, Saarbrücken, Germany — {theisel, hpseidel}@mpi-sb.mpg.de

Abstract

One of the reasons that topological methods have a limited popularity for the visualization of complex 3D flow fields is the fact that their topological structures contain a number of separating stream surfaces. Since these stream surfaces tend to hide each other as well as other topological features, for complex 3D topologies the visualizations become cluttered and hardly interpretable. One solution of this problem is the recently introduced concept of saddle connectors which treats separation surfaces emanating from critical points. In this paper we extend this concept to separation surfaces starting from boundary switch curves. This way we obtain a number of particular stream lines called boundary switch connectors. They connect either two boundary switch curves or a boundary switch curve with a saddle. We discuss properties and computational issues of boundary switch connectors and apply them to topologically complex flow data.

Categories and Subject Descriptors (according to ACM CCS): I.3.3 [Computer Graphics]: Line and Curve Generation I.3.3 [Computer Graphics]: Picture/Image Generation I.3.7 [Computer Graphics]: Three-Dimensional Graphics and Realism

1. Introduction

Topological methods are standard tools for the visualization of 2D vector fields. The main idea behind them is to segment the flow into areas of similar flow behavior. To do so, critical points and separatrices of the flow are extracted. Visualizing the topological skeleton is attractive since even a complex flow behavior can be represented by a limited number of graphical primitives.

After the introduction of topological methods to the visualization community in [HH89], an intensive research has been done in this field. [SKMR98] treat higher order critical points, i.e. critical points with a possibly vanishing Jacobian. In [dLvL99a], separatrices starting from boundary switch points are discussed. [WS01] gives a method to detect closed separatrices. Topological methods are used to simplify [dLvL99a, dLvL99b, TSH00, TSH01a], smooth [WJE01], compress [LRR00] and design [The02] vector fields. In [LBH98, BKH99, TW02], topology-based 2D vector field metrics are defined. The topological behavior of time-dependent vector fields is analyzed in [TSH01b, TWSH02, TS03].

Although the topology of 3D vector fields is well-understood in the visualization community, there are only a few applications which are based upon the topology of 3D vector fields. Similar to 2D vector fields, [HH91] proposed methods for detecting and classifying first order critical points by an eigenvalue/eigenvector analysis of the Jacobian matrix. A system for visualizing the topological skeleton of 3D vector fields has been presented in [GLL91]. Topological skeletons of particular analytic 3D vector fields are extracted in [LDG98, HG00]. Mahrous et. al ([MBS*02, MBHJ03]) obtain a topological segmentation of a vector field by sampling stream lines over the field and clustering areas where a similar inflow/outflow behavior of the stream lines is observed.

All 3D topology methods mentioned above either ignore separatrices, i.e. focus only on a part of the topology, or they were applied only to vector fields with a rather simple topology, i.e. with a small number of critical points, boundary switch curves and separatrices. One reason for this seems to be that separatrices of 3D vector fields consist also of stream surfaces – a fact which creates a number of problems. In

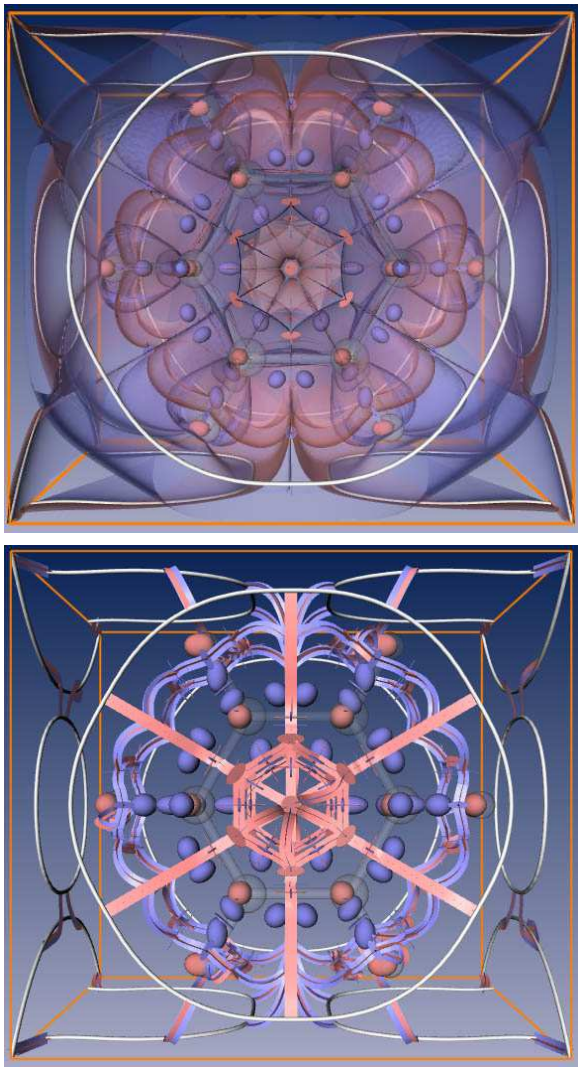

Figure 1: *Topological representations of the Benzene data set. (top) The topological skeleton looks visually cluttered due to the shown separation surfaces. (bottom) Visualization of the topological skeleton using connectors.*

particular, we see the following reasons why topological visualization of 3D vector fields is still less common than of 2D vector fields:

- The integration of stream surfaces is computationally more involved and less stable than the integration of stream lines, since convergence and divergence effects on the stream surface may occur.
- The visualization of the topological skeleton of a vector field requires the simultaneous visualization of a higher number of stream surfaces. These stream surfaces tend to hide each other and other topological features, leading to visually cluttered representations (Figure 1(top)).

A number of solutions have been proposed for the first problem, see [Hul92, Gel01, SBM*01, vW93].

A solution for the second problem was recently proposed in [TWHS03]. Here the separation surfaces starting from saddle points were considered. Instead of visualizing these stream surfaces, their intersection curves were extracted and visualized. [TWHS03] has shown that these intersection curves are particular stream lines which were called saddle connectors. The visualization of saddle connectors instead of the separation surfaces gave – for the first time – expressive visualizations even for topologically complex data sets.

Unfortunately, the solution in [TWHS03] was restricted to separation surfaces created by saddle points. If the boundary of the vector field is topologically considered as well, another class of separation surfaces becomes relevant: separation surfaces starting from boundary switch curves. These separation surfaces create similar problems as the ones starting from saddles: if a larger number of them is present, they tend to produce visually cluttered images (Figure 1(top)).

It is the purpose of this paper to extend the concept of saddle connectors to separation surfaces starting from boundary switch curves. We show that the intersections of these surfaces yield particular stream lines which will be called *boundary switch connectors*. We discuss their extraction and visualization and show that they give expressive topological visualizations even for data sets with a high number of boundary switch curves. Figure 1(bottom) illustrates an example.

The rest of the paper is organized as follows: section 2 reviews the theoretical background of 3D vector field topology including the concept of saddle connectors. In particular, section 2 introduces an enhanced iconic representation of the critical points in comparison to [TWHS03]. Section 3 discusses boundary switch curves and their classification into inbound and outbound segments. Section 4 introduces the concept of boundary switch connectors and discusses their extraction and visual representation. Section 5 demonstrates the application of boundary switch connectors to topologically complex 3D data sets, while conclusions are drawn in section 6.

2. Theoretical Background

Topological structures of 3D vector fields are well-understood in the visualization community for many years [HH91, Asi93, CPC90, PS97]. In this section, we collect the most important concepts and properties.

2.1. Critical Points

Consider a 3D vector field

$$\mathbf{v}(x,y,z) = \begin{pmatrix} u(x,y,z) \\ v(x,y,z) \\ w(x,y,z) \end{pmatrix}. \qquad (1)$$

A first order critical point $\mathbf{x}_0$ (i.e., $\mathbf{v}(\mathbf{x}_0) = \mathbf{0}$) can be classified by an eigenvalue/eigenvector analysis of the Jacobian matrix $\mathbf{J}_\mathbf{v}(\mathbf{x}) = \nabla\mathbf{v}(\mathbf{x})$, iff $\det(\mathbf{J}_\mathbf{v}(\mathbf{x}_0)) \neq 0$. Let $\lambda_1, \lambda_2, \lambda_3$ be the eigenvalues of $\mathbf{J}_\mathbf{v}(\mathbf{x}_0)$ ordered according to their real parts, i.e. $Re(\lambda_1) \leq Re(\lambda_2) \leq Re(\lambda_3)$. Furthermore, let $\mathbf{e}_1, \mathbf{e}_2, \mathbf{e}_3$ be the corresponding eigenvectors, and let $\mathbf{f}_1, \mathbf{f}_2, \mathbf{f}_3$ be the corresponding eigenvectors of the transposed Jacobian $(\mathbf{J}_\mathbf{v}(\mathbf{x}_0))^T$. (Note that $\mathbf{J}$ and $\mathbf{J}^T$ have the same eigenvalues but not necessarily the same eigenvectors.) The sign of the real part of an eigenvalue λ_i denotes – together with the corresponding eigenvector $\mathbf{e}_i$ – the flow direction: Positive values represent an *outflow* and negative values an *inflow* behavior. This leads to the following classification of first order critical points:

Sources:	$0 < Re(\lambda_1) \leq Re(\lambda_2) \leq Re(\lambda_3)$
Repelling saddles:	$Re(\lambda_1) < 0 < Re(\lambda_2) \leq Re(\lambda_3)$
Attracting saddles:	$Re(\lambda_1) \leq Re(\lambda_2) < 0 < Re(\lambda_3)$
Sinks:	$Re(\lambda_1) \leq Re(\lambda_2) \leq Re(\lambda_3) < 0$

Thus, sources and sinks consist of complete outflow/inflow, while saddles have a mixture of both. A repelling saddle has one direction of inflow behavior (called *inflow direction*) and a plane in which a 2D outflow behavior occurs (called *outflow plane*). Similar to this, an attracting saddle consists of an *outflow direction* and an *inflow plane*.

Each of the 4 classes above can be further divided into two stable subclasses by deciding whether or not imaginary parts in two of the eigenvalues are present ($\lambda_1, \lambda_2, \lambda_3$ are not ordered):

Foci:	$Im(\lambda_1) = 0 \quad \text{and} \quad Im(\lambda_2) = -Im(\lambda_3) \neq 0$
Nodes:	$Im(\lambda_1) = Im(\lambda_2) = Im(\lambda_3) = 0$

An iconic representation is an appropriate visualization for critical points, since vector fields usually contain a finite number of them. Several icons have been proposed in the literature, see [HH91, GLL91, LDG98, HG00, TWHS03]. Basically, we follow the design approach of [TWHS03] and color the icons depending on the flow behavior: Attracting parts (inflow) are colored blue, while repelling parts (outflow) are colored red (Figures 2 and 3).

In contrast to [TWHS03], we use elliptic cylinders instead of flat ellipses to depict the outflow/inflow planes of the saddles. We propose this change for a better three-dimensional perception of the icons by the user. Additionally, the icons can be much better distinguished from other topological features near them, like e.g. saddle connectors. This can be further enhanced by coloring them slightly darker or lighter. See Figure 4 for a comparison.

Higher order critical points are not considered in this paper.

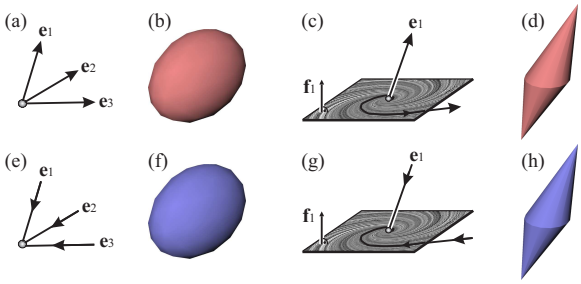

Figure 2: *Sources and sinks; (a) repelling node and (b) its icon; (c) repelling focus and (d) its icon; (e) attracting node and (f) its icon; (g) attracting focus and (h) its icon.*

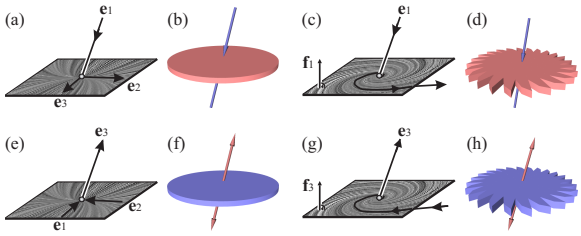

Figure 3: *Repelling and attracting saddles; (a) repelling node saddle and (b) its icon; (c) repelling focus saddle and (d) its icon; (e) attracting node saddle and (f) its icon; (g) attracting focus saddle and (h) its icon.*

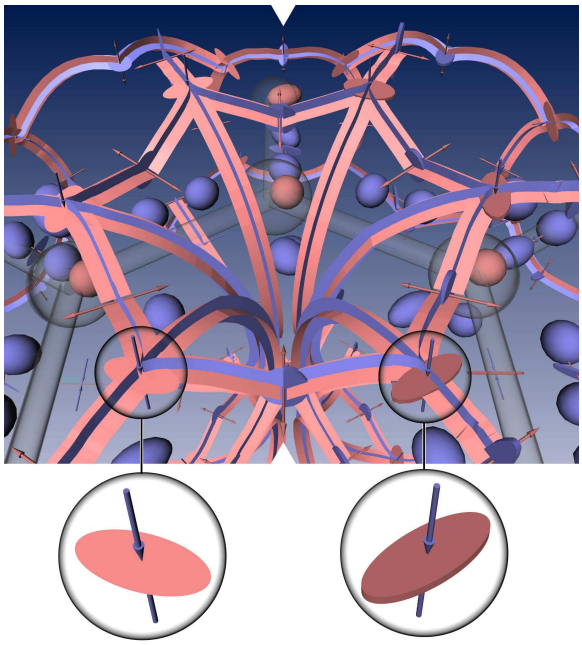

Figure 4: *Topological skeleton of the benzene data set showing saddle connectors and critical points. Left: Outflow/inflow planes of the saddle points depicted with flat ellipses. Right: Our enhanced design using elliptic cylinders.*

2.2. Separatrices

Separatrices are stream lines or stream surfaces which separate regions of different flow behavior. Different kinds of separatrices are possible: They can emanate from critical points, boundary switch curves, attachment and detachment lines, or they are closed separatrices without a specific emanating structure. However, in this paper we consider separatrices starting from critical points and boundary switch curves only.

Due to the homogeneous flow behavior around sources and sinks (either a complete outflow or inflow), they do not contribute to separatrices. Each saddle point creates two separatrices: Considering a repelling saddle $\mathbf{x}_R$, it creates one separation curve (which is a stream line starting in $\mathbf{x}_R$ in the inflow direction by backward integration) and a separation surface (which is a stream surface starting in the outflow plane by forward integration). A similar statement holds for attracting saddles.

Separatrices starting from boundary switch curves will be discussed in detail in section 3.

2.3. Saddle Connectors

Visualizing a rather complex topological skeleton involves showing a number of separation surfaces. This does not lead to visually pleasing results, because these surfaces hide most parts of the skeleton.

A solution of this problem is the appliance of saddle connectors, which were recently introduced in [TWHS03]. A saddle connector is the intersection curve of two separation surfaces, where one is emanating from a repelling and the other from an attracting saddle. This intersection curve is a stream line connecting both saddles, i.e. it starts at the repelling and ends at the attracting saddle.

[TWHS03] uses double flow ribbons for visulizing saddle connectors (Figure 4). Although this approach incorporates the local behaviour of the separation surfaces, one can no longer uniquely infer the flow behavior of $\mathbf{v}$ from any point of the domain. Therefore, [TWHS03] enables the user to interactively demand the display of *single* separation surfaces by simply clicking on a saddle connector.

3. Boundary Switch Curves

Consider the 3D vector field $\mathbf{v}$ from (1) in the domain

$$D = (x_{min}, x_{max}) \times (y_{min}, y_{max}) \times (z_{min}, z_{max}) \qquad (2)$$

with $x_{min} < x_{max}$, $y_{min} < y_{max}$, $z_{min} < z_{max}$. We assume that no critical point of $\mathbf{v}$ lies on the boundary surfaces of D. Furthermore, D might be the whole domain in which $\mathbf{v}$ is defined, or it may be interactively modified and moved around in the data set, leading to a "local topology" ([SHJK00]).

The boundary surfaces of D (which are the 6 faces of the bounding box) consist of outflow and inflow areas which are separated by *boundary switch curves*. Boundary switch curves consist of all points on the boundary where the flow direction is tangential to the boundary surface. Figure 5 illustrates an example of the boundary plane $z = z_{min}$ consisting of one inflow and one outflow area. (In the following we illustrate the concept of boundary switch curves only on the boundary plane $z = z_{min}$. Similar statements hold for the 5 remaining boundary planes of D.)

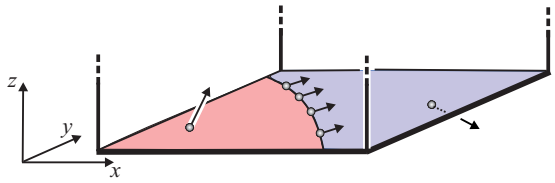

Figure 5: *Boundary plane $z = z_{min}$ consisting of an inflow area (blue), an outflow area (red), and their separating boundary switch curve; shown are 4 vectors of* $\mathbf{v}$ *on the boundary switch curve, and one each in the inflow and outflow area.*

In general, boundary switch curves do not intersect each other. The case of intersecting boundary switch curves can be considered to be structurally unstable: a small perturbation of $\mathbf{v}$ removes the intersection. Because of this, intersections of boundary switch curves are not considered here.

Given a point $\mathbf{p}_0$ on a boundary switch curve, two cases are possible concerning the stream line starting at $\mathbf{p}_0$:

- Starting from $\mathbf{p}_0$, the stream line integration moves inside D for both backward and forward integration. We call this point an *inbound point* on the boundary switch curve (Figure 6a).
- Starting from $\mathbf{p}_0$, the stream line integration moves outside D for both backward and forward integration. Therefore, this stream line in D consists only of $\mathbf{p}_0$ itself. We call this point an *outbound point* (Figure 6b).

To distinguish inbound from outbound points, two approaches can be used:

1. Decide whether $\mathbf{v}(\mathbf{p}_0)$ points into the inflow or the outflow area. If $\mathbf{v}(\mathbf{p}_0)$ points into the inflow area, $\mathbf{p}_0$ is an inbound point. If $\mathbf{v}(\mathbf{p}_0)$ points into the outflow area, $\mathbf{p}_0$ is an outbound point. This condition corresponds to the classification of boundary switch points for 2D vector fields given in [dLvL99a].
2. Consider the second derivative vector $\dot{\mathbf{v}}$ of the stream lines as a local property of $\mathbf{v}$ (assuming that the tangent vectors of the stream lines are given by $\mathbf{v}$). This gives

$$\dot{\mathbf{v}}(x,y,z) = \begin{pmatrix} \dot{u}(x,y,z) \\ \dot{v}(x,y,z) \\ \dot{w}(x,y,z) \end{pmatrix} = u\,\mathbf{v}_x + v\,\mathbf{v}_y + w\,\mathbf{v}_z.$$

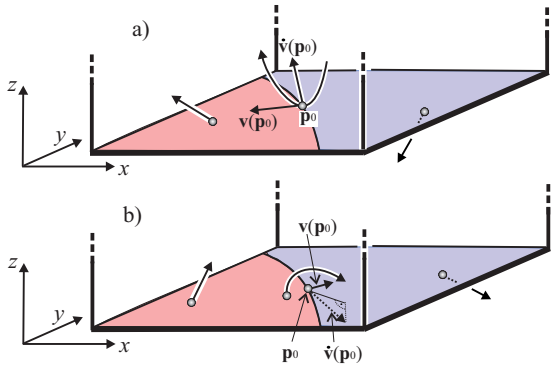

Figure 6: *a) inbound point $\mathbf{p}_0$ on a boundary switch curve: $\mathbf{v}(\mathbf{p}_0)$ points into the inflow area, $\dot{\mathbf{v}}(\mathbf{p}_0)$ points inside D; shown is a part of the stream line starting in $\mathbf{p}_0$ both in forward and backward integration; b) outbound point $\mathbf{p}_0$ on a boundary switch curve; $\mathbf{v}(\mathbf{p}_0)$ points into the outflow area, $\dot{\mathbf{v}}(\mathbf{p}_0)$ points outside D; shown is a stream line close to $\mathbf{p}_0$ starting in the inflow area and leaving D in the outflow area.*

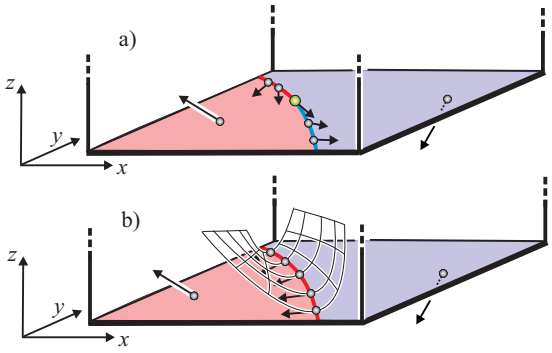

Figure 7: *a) boundary switch curve consisting of one inbound segment (dark red) and one outbound segment (dark blue); they are separated by an inout point (green); b) separation surface starting from an inbound segment in both forward and backward integration.*

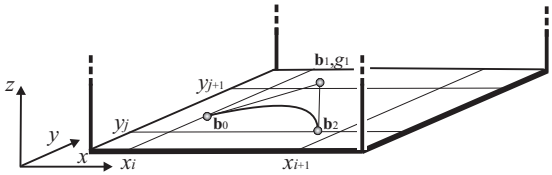

Figure 8: *Description of a hyperbolic segment as a piecewise rational quadratic Bézier curve.*

See [TF97] and [WT02] for details of this. ($\dot{\mathbf{v}}$ can for example be used to compute the curvature of the stream lines in every point of D: $\kappa = \frac{\|\mathbf{v}\times\dot{\mathbf{v}}\|}{\|\mathbf{v}\|^3}$.) Then $\mathbf{p}_0$ is an inbound point if $\dot{\mathbf{v}}(\mathbf{p}_0)$ points into D. If $\dot{\mathbf{v}}(\mathbf{p}_0)$ points out of D, $\mathbf{p}_0$ is an outbound point.

Figure 6 illustrates both criteria. It can be shown by a straightforward exercise in algebra that both criteria 1. and 2. are equivalent. We preferred to use condition 2., since for a domain D given in (2), it turns out to be simply a sign check of one component of $\dot{\mathbf{v}}$.

Inbound points and outbound points form *inbound segments* and *outbound segments* on the boundary switch curve. These segments are separated by *inout points*. A point $\mathbf{p}_0$ is an inout point if $\mathbf{v}(\mathbf{p}_0)$ is parallel to the tangent direction of the boundary switch curve in $\mathbf{p}_0$ (or equivalently, if $\dot{\mathbf{v}}(\mathbf{p}_0)$ lies in the tangent plane of the considered boundary of D). For a boundary switch curve, we extract all inout points and thus divide the curve into a number of inbound and outbound segments (Figure 7a).

The distinction between inbound segments and outbound segments plays an important role for the topological segmentation of a 3D vector field, because the inbound segments are the seeding curves of the separation surfaces emanating from the boundary of D. Figure 7b shows an example. Outbound segments do not contribute to separation surfaces in the 3D flow.

3.1. Extracting Boundary Switch Curves

Assuming $\mathbf{v}$ to be piecewise trilinear and $z = z_{min}$ being a grid plane of the underlying grid, the boundary switch curves are the zeros of the piecewise biquadratic scalar field $w(x,y,z_{min})$ from (1). It is a well-known fact that these isocurves consist of piecewise hyperbolas with G^0 continuous junction points. We extract and describe each hyperbolic curve segment as a rational quadratic Bézier curve $\mathbf{h}(t)$ described by the Bézier points $\mathbf{b}_0, \mathbf{b}_1, \mathbf{b}_2$ and the corresponding weights g_0, g_1, g_2 with $g_0 = g_2 = 1$. This way, $\mathbf{b}_0$ and $\mathbf{b}_2$ are the intersections of the curve with the grid lines (obtained by a linear interpolation), $\mathbf{b}_1$ is obtained as the intersection of the tangents at $\mathbf{b}_0$ and $\mathbf{b}_2$ (which are computed as the gradients of $w(x,y,z_{min})$), and g_1 is chosen such that $w(\mathbf{h}(t)) \equiv 0$. Figure 8 gives an illustration.

3.1.1. Finding Inbound and Outbound Segments on Boundary Switch Curves

If $\mathbf{v}$ is a piecewise trilinear vector field, all junction points of the piecewise hyperbolic segments are candidates for being an inout point. In addition, up to 4 inout points may exist inside a hyperbolic boundary switch curve segment. Therefore we have applied numerical methods to get the inout points and thus find the inbound and outbound segments.

If $\mathbf{v}$ is piecewise linear, then the boundary switch curves are piecewise linear curves, and inout points can be the junctions of the linear curve segments as well as up to one additional point inside each linear segment. This point can di-

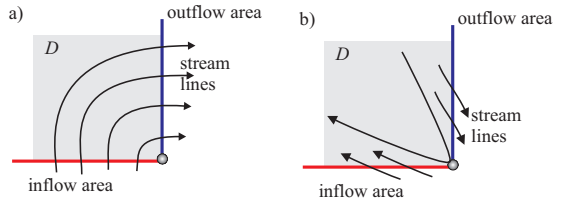

Figure 9: *a) boundary switch point on a vertex of the rectangular domain of a 2D vector field; b) inbound segments on the edges of D do not exist.*

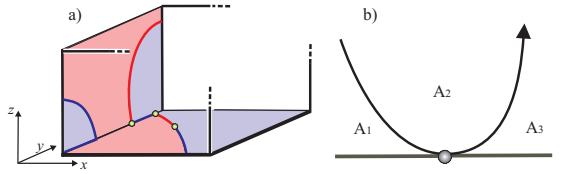

Figure 10: *a) inflow/outflow behavior on two faces of D creates two boundary switch curves on the shared edge; these boundary switch curves are always outbound segments; b) inbound boundary switch point divides D into 3 areas A_1, A_2, A_3.*

rectly be computed by solving a 2×2 system of linear equations.

3.1.2. Boundary Switch Curves on the Edges of *D*

Up to now we only considered boundary switch curves on the faces of *D* defined by (2). However, the edges of *D* are candidates for being boundary switch curves as well, since the two faces sharing an edge may have a different inflow/outflow behavior. (Figure 9a gives a 2D example of a boundary switch point on a vertex of a rectangular domain.) Hence, also the edges of *D* have to be checked for being boundary switch curves. This is done by computing the inflow/outflow behavior of the faces of *D* which share the edge. Figure 10a illustrates an example.

Boundary switch curves on edges are always outbound segments which therefore do not create separation surfaces. To show this, consider figure 9b. If a point on the edge of *D* is an inbound point, it must have a curvature diverging to infinity. Since this only happens for critical points [WT02] and critical points are not supposed to be on the boundary, an inbound segment on an edge cannot exist.

4. Boundary Switch Connectors

Each inbound segment of a boundary switch curve creates two separation surfaces: one is obtained by applying a forward integration starting from the boundary switch curve, the other one by backward integration. These two separation surfaces divide the flow into three areas of different inflow/outflow behavior. Figure 10 illustrates this for a 2D example. Unfortunately, the visualization of all those separation surfaces creates the same problems as [TWHS03] identified for separation surfaces starting from saddles: if a higher number of separation surfaces is present, their visualization tends to be cluttered due to various occlusion effects. Figure 1(top) illustrates this.

The solution for this problem we propose here is an extension of the idea in [TWHS03]: instead of visualizing the separation surfaces directly, we compute all intersection curves of these surfaces and visualize this skeleton of curves. In fact, here we choose a general approach which yields the intersection curves of all separation surfaces starting either from a saddle point or a boundary switch curve. Analyzing these curves, we obtain the following properties:

- The intersection curves of two separation surfaces are stream lines. This is due to the fact that the intersection of two stream surface is always a stream line (or degenerate).
- Each intersection curve starts either in the outflow plane of a repelling saddle, or on a boundary switch curve by integrating in forward direction.
- Each intersection curve ends either in the inflow plane of an attracting saddle or on a boundary switch curve by integrating in backward direction.

The latter two statements give the following classification regarding the intersection curves of the separation surfaces:

1. The curve starts in a repelling saddle and ends in an attracting saddle. (Figure 11a)
2. The curve starts in a repelling saddle and ends in a boundary switch curve. (Figure 11b)
3. The curve starts in a boundary switch curve and ends in an attracting saddle. (Figure 11c)
4. The curve starts in a boundary switch curve and ends in a different boundary switch curve. (Figure 11d)
5. The curve starts in a boundary switch curve and ends in the same boundary switch curve. (Figure 11e)

Case 1. has been treated in [TWHS03]. Since these curves start and end in two saddles, [TWHS03] calls them saddle connectors. In this paper we particularly focus on the cases 2.–5. and since all these curves start or end in boundary switch curves, we call them *boundary switch connectors*. Therefore, the main idea of our approach is to extract all saddle connectors and all boundary switch connectors of a vector field and visualize them.

When intersecting two separation surfaces, the result may be not a curve but a surface as well. We consider this as a degenerate case which we do not take into account here. However, note that the intersection of two separation surfaces may give more than one single intersection curve.

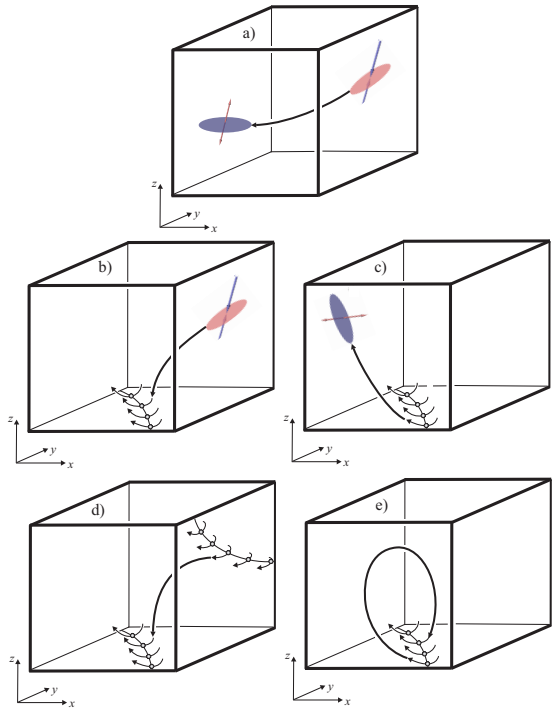

Figure 11: *Cases of intersection curves of separation surfaces: a) saddle connectors; b)-e) boundary switch connectors.*

4.1. Computing Boundary Switch Connectors

Boundary switch connectors are a global feature of a 3D vector field. A naive approach to extract them is to numerically integrate all separation surfaces and intersect the resulting triangle meshes to get a polygonal representation of the connectors. This approach has turned out to have limitations concerning accuracy and memory requirements. So we use an algorithm which makes use of the fact that the intersection of two separation surfaces is a stream line. Such an algorithm was described in [TWHS03] to extract saddle connectors. Fortunately, this algorithm can directly be extended to extract boundary switch connectors. Se we describe the main idea here and refer to [TWHS03] for the details.

To find the intersection between a separation surface in forward integration and a separation surface in backward integration, we integrate both separation surfaces simultaneously until a first intersection point $\mathbf{p}_1$ is found. After refining this intersection point (see [TWHS03] for details), a stream line from $\mathbf{p}_1$ is integrated both forwards and backwards. This stream line is the boundary switch connector. Figure 12 gives an illustration of this algorithm.

After finding a first boundary switch connector, both separation surfaces are continued to be integrated to find further intersections which are not covered yet by the first boundary switch connector. If such a new intersection point $\mathbf{p}_2$ is found, a new boundary switch connector is obtained from $\mathbf{p}_2$. This process stops when one of the following conditions are fulfilled:

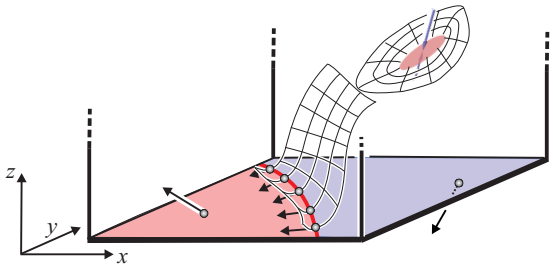

Figure 12: *Finding the intersection of two separation surfaces – one comes from a saddle, while the other one comes from a boundary switch curve; shown is the situation short before an intersection is found; in the next integration step an intersection point $\mathbf{p}_1$ is found which defines the boundary switch connector.*

- One of the separation surfaces completely leaves D or degenerates to a number of critical points.
- The maximal number n_{max} of boundary switch connectors between two separation surfaces is found, or the maximal number t_{max} of integration steps has been reached. n_{max} and t_{max} have to be set by the user.

To obtain all boundary switch connectors, we simultaneously integrate all separation surfaces and check for intersections. If an intersection between any two of them is found, a boundary switch connector is constructed from this intersection point. A separation surface is excluded from this process if it leaves D or collapses to critical points.

4.2. Visual Representation of Boundary Switch Connectors

Since boundary switch connectors are stream lines, a visual representation for instance as illuminated stream lines ([ZSH96]) is possible. However, we want to emphasize the fact that such stream lines are obtained as the intersection of two separation surfaces. Hence we choose a double stream ribbon representation to additionally show the orientation of the intersecting surfaces in each point of the stream line. To do so, a second curve has to be constructed close to the boundary switch connector. Then the ribbon is constructed between the second curve and the boundary switch connector. To get this curve, two problems have to be solved:

1. An appropriate starting point has to be found close to the starting point of the original boundary switch connector.
2. A simultaneous stream line integration and correction of the distance to the boundary switch connector has to be applied to keep both curves in the same distance to each other.

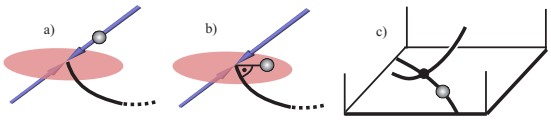

Figure 13: *Starting points (grey balls) for the double flow ribbon integration; a) for saddle connectors; b) for boundary switch connectors starting in a saddle; c) for boundary switch connectors starting on a boundary switch curve.*

An algorithm solving these problems for saddle connectors was proposed in [TWHS03]. Here we use a modification of this. In fact, for step 1. we need a different approach, since [TWHS03] starts the additional integration on a point in the inflow/outflow direction of the saddles (Figure 13a). For boundary switch connectors, we have to choose the starting point in a different way: if the separation surface starts in a saddle, we place the starting point into the inflow/outflow plane, perpendicular to the direction of the boundary switch connector, with a certain predefined distance ε to the saddle point (Figure 13b). If the boundary switch connector starts from a boundary switch curve, the starting point is located on the boundary switch curve in a certain distance ε to the starting point of the connector (Figure 13c).

5. Applications

We applied the concept of boundary switch connectors to two 3D data sets of a rather complex topology.

Figures 14a–d visualize a snapshot of a transitional wake behind a circular cylinder [ZFN*95]. This flow exhibits periodic vortex shedding leading to the well known von Kármán vortex street. This phenomenon plays an important role in many industrial applications, like mixing in heat exchangers or mass flow measurements with vortex counters. However, this vortex shedding can lead to undesirable periodic forces on obstacles, like chimneys, buildings, bridges and submarine towers.

This data set was derived from a direct numerical simulation of the Navier-Stokes equation by Gerd Mutschke [Mut03]. The data resolves the so-called 'mode A' of the 3D transition at a Reynolds number of 200 and at a spanwise wavelength of 4 diameters. The figures display a small near-wake region of a large computational domain. All 13 critical points are contained in the shown domain and on its boundaries 13 boundary switch curves are observed. Together they span the topological skeleton of the incompressible velocity field.

The inspection of figure 14a suggests a high amount of circulating flow behaviour in the data set, but due to the occlusion effects introduced by the separation surfaces neither the flow behaviour on the boundaries nor the critical points can be seen easily. This complicates further examinations to a high degree.

detected features	Benzene	Cylinder
critical points (**A** / **R** saddles)	184 (78 / 43)	13 (7 / 6)
BS curves / inbound segments	12 / 16	13 / 22
A / **R** separation surfaces	94 / 59	29 / 28
connectors (overall)	181	59
BS connectors **B** ↔ **B** / **B** ↔ **Sa**	24 / 28	29 / 21
saddle connectors	129	9

Table 1: *Number of features detected by our algorithms.*

The simplified topological skeletons shown in Figures 14b–d enable to reduce this high-dimensional data set to a simple conceptual flow representation from which qualitative conclusions can be drawn. Using connectors, the skeleton elucidates the symmetry of the mode A with respect to a plane which is perpendicular to the cylinder axis. The high number of spanwise and transverse running connectors of a single snapshot already indicate the experimentally observed good mixing properties of vortex shedding.

Figure 1 visualizes the electrostatic field around a benzene molecule. This data set was calculated on a 101^3 regular grid using the fractional charges method described in [SS96]. For this visualization we used a smaller subdomain around the molecule itself. All 184 critical points are inside the shown region.

Table 1 gives a summary of the data sets and shows the topological richness of both. These examples show that boundary switch and saddle connectors give expressive visualizations even for topologically complex 3D vector fields.

6. Conclusions

In this paper we have introduced the concept of boundary switch connectors as a new approach to visualizing the topological skeleton of complex 3D vector fields. Boundary switch connectors are particular stream lines which connect boundary switch curves with either a saddle or another boundary switch curve. They can be considered as a generalization of saddle connectors ([TWHS03]) which connect two saddles.

We described all cases of boundary switch connectors. To extract them, we used an extension of the algorithm for extracting saddle connectors. For the visual representation we have chosen a double stream ribbon approach which needed – compared to [TWHS03] – a new choice of the starting point of the ribbon integration. Furthermore, we gave an enhanced iconic representation of saddle points by using elliptic cylinders instead of flat ellipses.

Similar to saddle connectors, boundary switch connectors

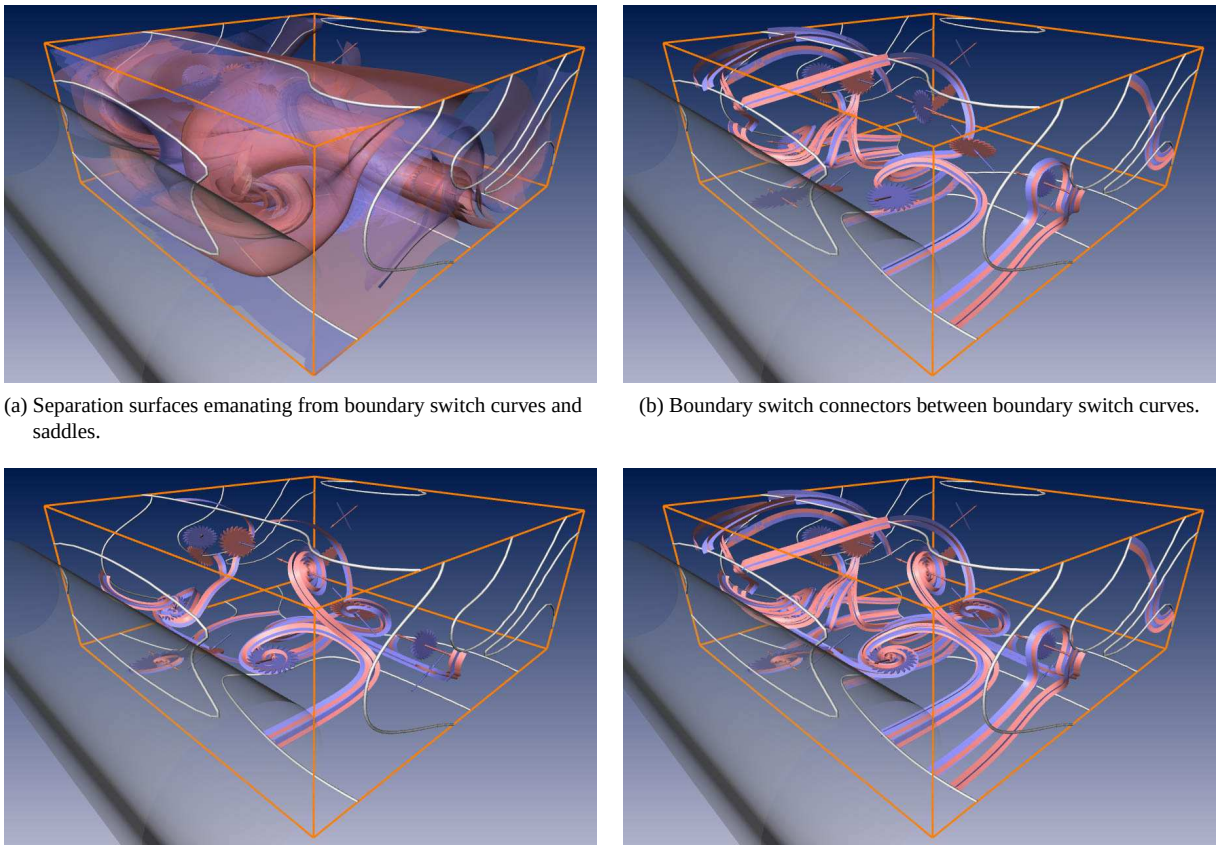

(a) Separation surfaces emanating from boundary switch curves and saddles.

(b) Boundary switch connectors between boundary switch curves.

(c) Boundary switch connectors between saddle points and boundary switch curves.

(d) Saddle connectors and both types of boundary switch connectors.

Figure 14: *Flow behind a circular cylinder. Different topological representations.*

can be interpreted as a "skeleton of a skeleton" approach which computes and visualizes a geometrically simplified representation of the system of separation surfaces. We have shown that the application of boundary switch connectors gives expressive visualizations even for topologically complex flow areas, i.e. areas where many critical points and boundary switch curves are present.

Acknowledgements

We thank Bernd R. Noack for the fruitful discussions and supply of simulation data which was kindly provided by Gerd Mutschke. All visualizations in this paper have been created using AMIRA – a system for advanced 3D visualization and volume modeling [SHW04] (see `http://amira.zib.de/`).

References

[Asi93] ASIMOV D.: *Notes on the topology of vector fields and flows*. Tech. rep., NASA Ames Research Center, 1993. RNR-93-003.

[BKH99] BATRA R., KLING K., HESSELINK L.: Topology based vector field comparison using graph methods. In *Proc. IEEE Visualization '99, Late Breaking Hot Topics* (1999), pp. 25–28.

[CPC90] CHONG M. S., PERRY A. E., CANTWELL B. J.: A general classification of three-dimensional flow fields. *Physics of Fluids A 2*, 5 (1990), 765–777.

[dLvL99a] DE LEEUW W., VAN LIERE R.: Collapsing flow topology using area metrics. In *Proc. IEEE Visualization '99* (1999), pp. 149–354.

[dLvL99b] DE LEEUW W., VAN LIERE R.: Visualization of global flow structures using multiple levels of topology. In *Data Visualization 1999. Proc. VisSym 99* (1999), pp. 45–52.

[Gel01] GELDER A. V.: Stream surface generation for fluid flow solutions on curvilinear grids. In *Data Visualization 2001. Proc. VisSym 01* (2001).

[GLL91] GLOBUS A., LEVIT C., LASINSKI T.: A tool for visualizing the topology of three-dimensional vector fields. In *Proc. IEEE Visualization '91* (1991), pp. 33–40.

[HG00] HAUSER H., GRÖLLER E.: Thorough insights by enhanced visualization of flow topology. In *9th international symposium on flow visualization* (2000).

[HH89] HELMAN J., HESSELINK L.: Representation and display of vector field topology in fluid flow data sets. *IEEE Computer 22*, 8 (August 1989), 27–36.

[HH91] HELMAN J., HESSELINK L.: Visualizing vector field topology in fluid flows. *IEEE Computer Graphics and Applications 11* (May 1991), 36–46.

[Hul92] HULTQUIST J.: Constructing stream surfaces in steady 3D vector fields. In *Proc. IEEE Visualization '92* (1992), pp. 171–177.

[LBH98] LAVIN Y., BATRA R., HESSELINK L.: Feature comparisons of vector fields using earth mover's distance. In *Proc. IEEE Visualization '98* (1998), pp. 103–109.

[LDG98] LÖFFELMANN H., DOLEISCH H., GRÖLLER E.: Visualizing dynamical systems near critical points. In *Spring Conference on Computer Graphics and its Applications* (1998), pp. 175–184.

[LRR00] LODHA S., RENTERIA J., ROSKIN K.: Topology preserving compression of 2D vector fields. In *Proc. IEEE Visualization 2000* (2000), pp. 343–350.

[MBHJ03] MAHROUS K., BENNETT J., HAMANN B., JOY K.: Improving topological segmentation of three-dimensional vector fields. In *Data Visualization 2003. Proc. VisSym 03* (2003), pp. 203–212.

[MBS*02] MAHROUS K., BENNETT J., SCHEUERMANN G., HAMANN B., JOY K.: *Topological Segmentation in Three-dimensional Vector Fields*. Tech. Rep. 36, Computer Science Department, University of California, Davis, 2002.

[Mut03] MUTSCHKE G.:, 2003. private communication.

[PS97] PHILIPPOU P. A., STRICKLAND R. N.: Vector field analysis and synthesis using three dimensional phase portraits. *Graphical Models and Image Processing 59* (November 1997), 446–462.

[SBM*01] SCHEUERMANN G., BOBACH T., MAHROUS H. H. K., HAMANN B., JOY K., KOLLMANN W.: A tetrahedra-based stream surface algorithm. In *Proc. Visualization 01* (2001), pp. 151 – 158.

[SHJK00] SCHEUERMANN G., HAMANN B., JOY K., KOLLMAN W.: Visualizing local vector field topology. *SPIE Journal of Electronic Imaging 9*, 4 (2000), 356–367.

[SHW04] STALLING D., HEGE H.-C., WESTERHOFF M.: Amira – a highly interactive system for visual data analysis. In *Visualization Handbook* (2004), Johnson C. R., Hansen C. D., (Eds.), Academic Press.

[SKMR98] SCHEUERMANN G., KRÜGER H., MENZEL M., ROCKWOOD A.: Visualizing non-linear vector field topology. *IEEE Transactions on Visualization and Computer Graphics 4*, 2 (1998), 109–116.

[SS96] STALLING D., STEINKE T.: *Visualization of Vector Fields in Quantum Chemistry*. Tech. rep., ZIB Preprint SC-96-01, 1996.

[TF97] THEISEL H., FARIN G.: The curvature of characteristic curves on surfaces. *IEEE Computer Graphics and Applications 17*, 6 (1997), 88–96.

[The02] THEISEL H.: Designing 2D vector fields of arbitrary topology. *Computer Graphics Forum (Eurographics 2002) 21*, 3 (2002), 595–604.

[TS03] THEISEL H., SEIDEL H.-P.: Feature flow fields. In *Data Visualization 2003. Proc. VisSym 03* (2003), pp. 141–148.

[TSH00] TRICOCHE X., SCHEUERMANN G., HAGEN H.: A topology simplification method for 2D vector fields. In *Proc. IEEE Visualization 2000* (2000), pp. 359–366.

[TSH01a] TRICOCHE X., SCHEUERMANN G., HAGEN H.: Continuous topology simplification of planar vector fields. In *Proc. Visualization 01* (2001), pp. 159 – 166.

[TSH01b] TRICOCHE X., SCHEUERMANN G., H.HAGEN: Topology-based visualization of time-dependent 2D vector fields. In *Data Visualization 2001. Proc. VisSym 01* (2001), pp. 117–126.

[TW02] THEISEL H., WEINKAUF T.: Vector field metrics based on distance measures of first order critical points. In *Journal of WSCG* (2002), vol. 10:3, pp. 121–128.

[TWHS03] THEISEL H., WEINKAUF T., HEGE H.-C., SEIDEL H.-P.: Saddle connectors - an approach to visualizing the topological skeleton of complex 3D vector fields. In *Proc. IEEE Visualization 2003* (2003), pp. 225–232.

[TWSH02] TRICOCHE X., WISCHGOLL T., SCHEUERMANN G., H.HAGEN: Topology tracking for the visualization of time-dependent two-dimensional flows. *Computers & Graphics 26* (2002), 249–257.

[vW93] VAN WIJK J.: Implicit stream surfaces. In *Proc. Visualization 93* (1993), pp. 245–252.

[WJE01] WESTERMANN R., JOHNSON C., ERTL T.: Topology-preserving smoothing of vector fields. *IEEE Transactions on Visualization and Computer Graphics 7*, 3 (2001), 222–229.

[WS01] WISCHGOLL T., SCHEUERMANN G.: Detection and visualization of closed streamlines in planar flows. *IEEE Transactions on Visualization and Computer Graphics 7*, 2 (2001), 165–172.

[WT02] WEINKAUF T., THEISEL H.: Curvature measures of 3D vector fields and their applications. In *Journal of WSCG* (2002), vol. 10:2, pp. 507–514.

[ZFN*95] ZHANG H.-Q., FEY U., NOACK B., KÖNIG M., ECKELMANN H.: On the transition of the cylinder wake. *Phys. Fluids 7*, 4 (1995), 779–795.

[ZSH96] ZÖCKLER M., STALLING D., HEGE H.: Interactive visualization of 3D-vector fields using illuminated stream lines. In *Proc. IEEE Visualization '96* (1996), pp. 107–113.